Dynamics of sensorimotor plasticity during exoskeletal finger augmentation

Authors:
Dominika Radziun,[1]*† Siebe Geurts,[1]† Valeria C. Peviani,[1]‡ Luke E. Miller[1]‡

[1]Donders Institute for Brain, Cognition and Behaviour, Radboud University, Nijmegen, the Netherlands

*Corresponding author. Email: dominika.radziun@donders.ru.nl
†,‡ = These authors contributed equally to this work

Abstract
How does the brain integrate artificial body extensions into its somatosensory representations? Prior work shows that the body and technology are represented simultaneously, but little is known about how these representations evolve dynamically across different sensorimotor interaction phases. To fill this gap, we investigated the dynamics of somatosensory plasticity using a custom-built exoskeletal device that extended users' fingers by 10 cm. Across four time points, before, during (pre- and post-use), and after exoskeleton wear, participants completed a high-density proprioceptive mapping task to measure representations of biological and exoskeletal fingers. We observed three distinct phases of plasticity. First, wearing the exoskeleton led to a contraction of the perceived length of the biological finger. Second, after active use, the represented lengths of the biological and exoskeletal fingers stretched significantly, an effect absent when participants trained with a non-augmenting control device. Third, a post-removal aftereffect on the biological finger representation was observed. These results demonstrate that wearable augmentations are rapidly integrated into body representations, with dynamic proprioceptive adjustments shaped by structural and functional properties of the device. This work advances our understanding of how the sensorimotor system accommodates artificial extensions and highlights the potential for body-augmenting technologies to be intuitively integrated within the sensorimotor system.

Keywords
Body representation; Somatosensory plasticity; Wearable augmentation; Proprioception; Sensorimotor augmentation

Introduction

The human body is remarkably adaptable, capable of integrating artificial enhancements that extend its physical capabilities (Miller and Farnè, 2024). This includes traditional tools (e.g., rakes) that operate outside the body as well as body augmentation devices that directly interface with the user, including supernumerary robotic limbs (SRLs), extra digits, and articulated hand or arm exoskeletons (Prattichizzo et al., 2021; Yang et al., 2021). Decades of research has found that tools influence the user's body representations and their implementation in the brain (Maravita and Iriki, 2004; Martel et al., 2016). In contrast, relatively little is known about how body augmentation devices themselves are represented by the user's somatosensory system. Furthermore, most studies have used pre-post experimental designs, offering a limited temporal window into the effects of technology. In our study, we aimed to address these gaps by investigating how representations of the body and technology dynamically evolve across different interaction phases.

Both tools and augmentation devices drive changes in the user's body representations (Berti and Frassinetti, 2000; Eden et al., 2022; Gallivan et al., 2013; Holmes and Spence, 2004; Iriki et al., 1996; Longo and Serino, 2012; Miller et al., 2019b; Peviani et al., 2024). Tools alter their user's spatial tactile perception and motor kinematics in ways consistent with stretching the sensorimotor representation of the user's arm (Bruno et al., 2019; Canzoneri et al., 2013; Cardinali et al., 2011, 2009; Galigani et al., 2020; Garbarini et al., 2015; Martel et al., 2019; Miller et al., 2017, 2014; Najafabadi et al., 2023; Romano et al., 2019; Sposito et al., 2012). Beyond tools, a broad class of articulated augmentations—SRLs mounted at the shoulder or waist, exo-digits, and multi-DOF hand exoskeletons—expand the user's motor control abilities (Abdi et al., 2016; Hussain et al., 2016; Maekawa et al., 2020; Mooney and Herr, 2016; Penaloza and Nishio, 2018; Prattichizzo et al., 2021; Shafti et al., 2021; Umezawa et al., 2022; Yang et al., 2021). Controlling an extra robotic finger can modify body representation in sensorimotor cortices (Kieliba et al., 2021), aligning with evidence that tool use modulates somatosensory processing and induces plasticity in body representations, particularly in secondary somatosensory and posterior parietal cortices (Miller et al., 2019b).

The human nervous system can use proprioceptive feedback to extract the spatial extent of hand-held tools (Debats et al., 2017; Fabio et al., 2024; Miller et al., 2018; Peviani et al., 2024; Solomon and Turvey, 1988; Themelis et al., 2025). This suggests that the sensorimotor system constructs spatial representations of tools using similar computations as for the body (Miller et al., 2023). Evidence that the somatosensory system also represents the spatial extent of body augmentation technology is limited (Dowdall et al., 2025; Nishida et al., 2020). Furthermore, it is an open question whether—like the body—representations of technology undergo spatial plasticity (e.g., stretching) during motor learning—similar dynamics would be expected if body and technology were represented similarly.

The majority of the above studies assessed plasticity only before and after use, typically once the device was removed from the body. How body representations evolve while the technology is being worn and used has received little attention. Furthermore, the extent to which representations of biological and artificial segments are concurrently represented and interact remains unclear. Therefore, identifying the influence of technological augmentation at all distinct stages—from the initial wearing of the technology to its use and subsequent removal—is crucial for understanding the dynamics of plasticity.

To characterize the temporal dynamics of plasticity, we developed a passive, non-articulated exoskeletal device that directly interfaced with and extended the user's fingers. Participants completed a proprioceptive localization task (Peviani et al., 2024) over four stages: before and after wearing the exoskeleton, and before and after performing motor training tasks that required functional use of the device. This high-density proprioceptive localization task measured how accurately participants could localize different parts of their finger and the exoskeleton in space, allowing us to quantify changes in body representations at different time points. By sampling these distinct interaction phases and jointly mapping biological and exoskeletal segments, our approach significantly extends prior demonstrations of body-representation plasticity and sensorimotor remapping with a time-resolved account of how augmentation is integrated.

We observed three time-specific heterogenous effects of the exoskeletal fingers: (i) an initial compression of the user's biological finger representation upon wearing the device, (ii) a stretch of proprioceptive representations of both the user's biological and exoskeletal fingers that was driven by training to use the augmentative device—an effect that was absent after using a non-augmenting device, and (iii) a stretch of the user's finger representation that persisted after the device was removed and was likely driven by persistent exposure to wearing the exoskeleton. Together, these findings offer theoretically important insight into how the brain dynamically integrates artificial extensions into the body representations.

Results

Experiment 1A: Introduction to task protocols and exoskeleton familiarization

The goal of our study was to elucidate the temporal dynamics of somatosensory representational plasticity during body augmentation. To this end, we explored the effects of finger-length augmentation on somatosensory finger representation. Participants (n=18) performed a high-density proprioceptive localization task in which they used their left hand to indicate on a touchscreen where they felt specific target locations on their right index finger, which remained hidden under the screen. The task involved repeated localization of seven equally spaced points along the length of the finger (and later, also the exoskeleton), enabling fine-grained assessment of perceived spatial structure.

This task was performed at various time points relative to learning to use a finger-extending exoskeleton: before wearing the exoskeleton (stage 1); while wearing the exoskeleton, before using it (stage 2); while wearing the exoskeleton, after using it (stage 3); and after the exoskeleton was removed (stage 4). In all stages, we mapped the participant's representation of their biological index finger. In stages 2 and 3, we also concurrently mapped the participant's exoskeletal finger representation. Reported p-values are Bonferroni-corrected to account for five planned comparisons.

The finger-extending exoskeleton (Fig. 1A) is a 3D-printed structure that elongates the fingers of the user's right hand by 10 cm, mounted on the biological fingertips. Their structure was designed to mimic the biological fingers. It consisted of a central rigid component intended to mimic the bone, surrounded by a padded silicon coating intended to mimic the elasticity of the finger pads and surrounding tissue. The latter ensured greater mechanical compliance during object manipulation, improving the user's success. Crucially, the finger-extending exoskeletal device was designed to explicitly allow us to simultaneously measure spatial perception of both the biological and exoskeletal fingers.

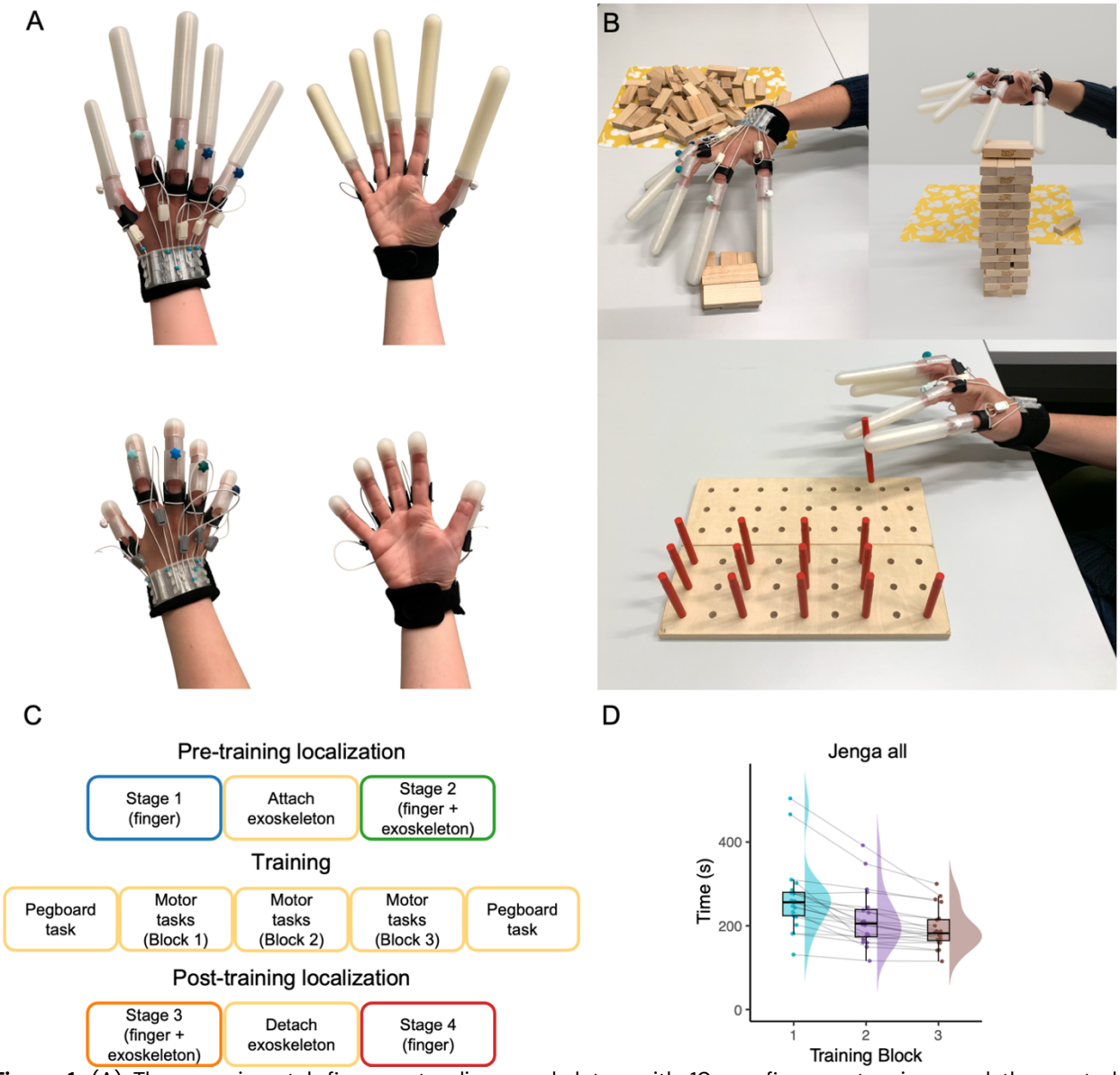

Figure 1. (A) The experimental, finger-extending exoskeleton with 10 cm finger extensions and the control exoskeleton without the extensions. (B) Example of the Jenga stacking training task. Participants wore the exoskeleton and were asked to stack a full Jenga tower; task performance was measured by the time taken to complete the tower. (C) Outline of the experimental design. (D) Group data showing improvement in performance (reduction in completion time) across training blocks.

Wearing the exoskeleton contracts perceived biological finger length

Participants initially localized seven proprioceptive targets—equally spaced along the midline of the right index finger from the base to the fingertip—by touching the corresponding locations on a touchscreen (stage 1). Each target was judged 20 times and the perceived location for each target was the mean of those repetitions (see also Fig. S2A for the target layout). We then used linear regression to characterize their biological finger representation, modelling their localization judgments as a function of actual target location. This analysis revealed that participants'

representation was geometrically accurate, with regression slopes near one (i.e., full accuracy; mean±sem: 1.06±0.09, 95% CI [0.86, 1.25]).

Participants were then fit with the exoskeletal fingers, providing them a short period of visual and proprioceptive feedback about their mechanics and geometry (around 1-2 minutes). They then performed the proprioceptive localization task while wearing the exoskeletons (stage 2). The mapping now included 14 targets: seven on the biological finger and seven on the exoskeletal segment (Fig. S2B). Importantly, the task mapped both the biological and exoskeletal fingers simultaneously (bio+exo).

When wearing the exoskeletal fingers, the combined bio-exoskeleton map was geometrically accurate, spanning the true length of the combined surface (true length: 17.40 cm; estimated length: 18.92 cm; paired *t*-test of map versus true length: $t(17) = -1.25$, $p = .23$, $BF_{10} = 0.48$). How this space was partitioned up, however, was not proportional across surfaces. Specifically, the biological finger segment was significantly under-represented compared to the exoskeletal segment (bio slope mean±sem: 0.85±0.06; exo slope mean±sem: 1.17±0.08; two-tailed paired t-test: $t(17) = -4.37$, $p = .002$, $BF_{10} = 79.66$), only making up 35.25% of the representation (actual: 42.5%). Comparison of the biological finger slopes with the map measured during stage 1 demonstrated that attaching the exoskeletal finger significantly contracted the represented length of the biological finger (19.65% reduction; $t(17) = 2.94$, $p = .046$, $BF_{10} = 5.66$).

Active use of the exoskeleton leads to proprioceptive "stretching" of biological and artificial finger segments

After stage 2, participants completed a 30-45 minute training period to familiarize themselves with the exoskeletal fingers. Training performance improved significantly over time, indicating a clear learning effect and increased proficiency with the device (Fig. 1D). Detailed analyses of individual tasks consistently showed significant improvements across sessions, confirming this effect. Full statistical results and task-specific analyses are provided in the Supplementary Information.

Following training, participants again completed the bio+exo finger localization task (stage 3). Based on previous research with tool use (Bruno et al., 2019; Canzoneri et al., 2013; Cardinali et al., 2011, 2009; Galigani et al., 2020; Garbarini et al., 2015; Martel et al., 2019; Miller et al., 2017, 2014; Najafabadi et al., 2023; Romano et al., 2019; Sposito et al., 2012), we hypothesized that training would stretch the user's finger representation. We found that participants' internal mapping of the combined finger (biological + exoskeleton) was no longer geometrically accurate (true length: 17.40 cm; estimated length: 21.18 cm; paired t-test: $t(17) = -3.09$, $p = .007$, $BF_{10} = 7.38$). This served as an initial confirmation of our hypothesis that training with the exoskeleton led to a representational stretch.

We then examined how proprioception of both the biological finger and the artificial exoskeleton segment changed following functional augmentation. The

perceived length of the biological finger following training (slope mean±sem: 1.00±0.07, 95% CI [0.86, 1.14]) was significantly longer after training (17.89% increase; $t(17) = 3.67$, $p = .009$ $BF_{10} = 21.65$), demonstrating that finger augmentation stretched the user's finger representation. Interestingly, we identified a similar effect of representational stretch for user's representation of the exoskeletal finger (slope mean±sem: 1.35±0.08, 95% CI [1.19, 1.52]; length change: 15.33% increase; $t(17) = 3.77$, $p = .008$, $BF_{10} = 26.01$). Though stretched, the relative portion of the representation devoted to the finger remained stable (finger proportion 35.22%; paired t-test on proportions before and after training: $t(17) = 0.02$, $p = .96$, $BF_{01} = 4.11$). Together, these findings indicate that proprioceptive representations of both the biological and artificial segments were stretched following training with the finger-extending exoskeleton.

Proprioceptive aftereffects emerge following exoskeleton exposure

After completing the bio+exo localization task (stage 3), participants performed the localization task again with the exoskeleton removed (stage 4). This allowed us to examine whether representational changes to the biological finger remained at this immediate, post-removal measurement. We did this by comparing the final representation length, measured in stage 4 (slope mean±sem: 1.32±0.08, 95% CI [1.16, 1.49]), with two previous stages: stage 1 and stage 3. Regardless of which set of stages we compared the final mapping to, we observed a similar a modulation in the length of the participant's biological finger representation: an 25.35% increase compared to stage 1 (Fig. 2C; paired t-test: $t(17) = -5.15$, $p < .001$, $BF_{10} = 345.48$); and an increase of 32.33% compared to stage 3 (Fig. 2D; $t(17) = -4.56$, $p = .001$, $BF_{10} = 113.70$).

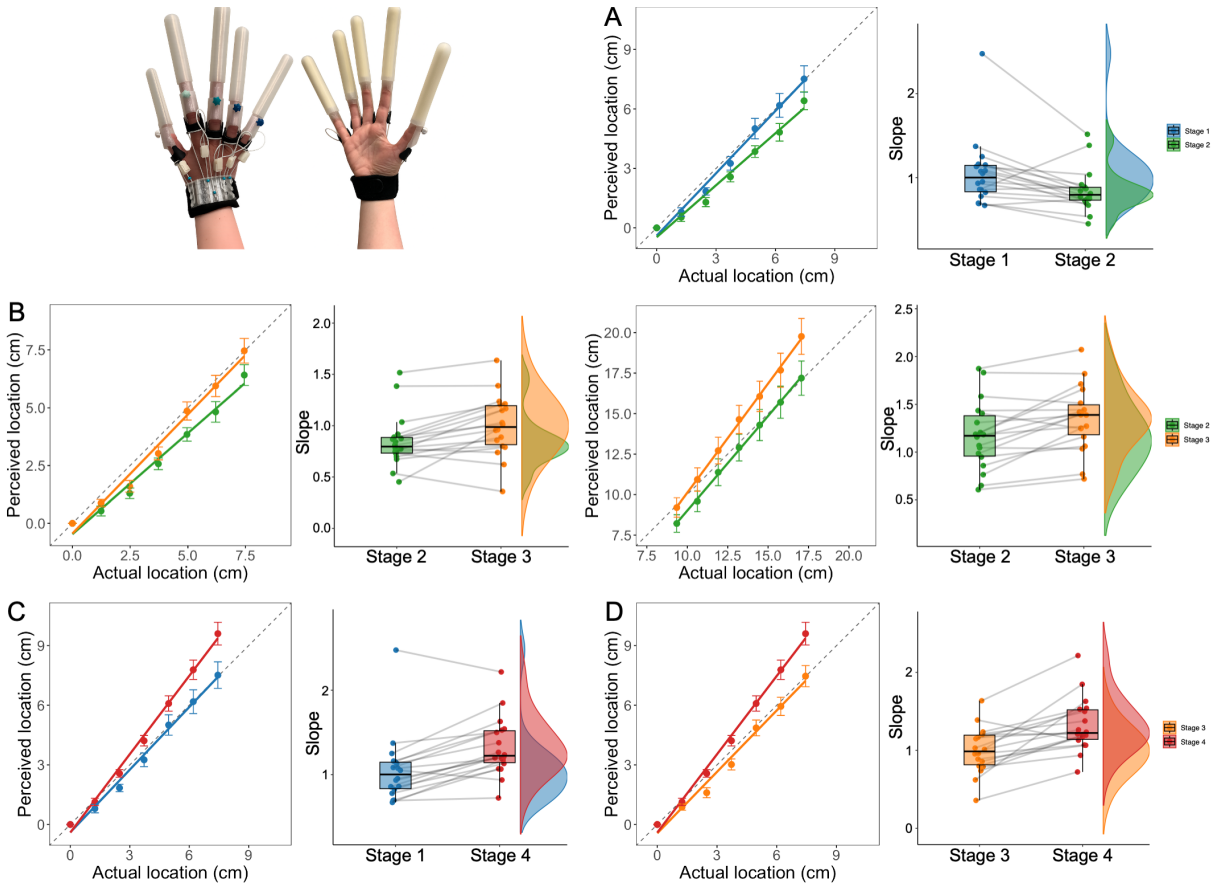

Figure 2. Proprioceptive judgments across stages of augmentation with finger-extending exoskeleton. (A) Comparison of proprioceptive maps from stage 1 (baseline) and stage 2 (initial exoskeleton fitting). (B) Left: Comparison of biological finger segment between stage 2 and stage 3 (after training). Right: Comparison of artificial finger segment between the same stages. (C) Comparison of biological finger representation from stage 1 to stage 4 (post-exoskeleton removal). (D) Comparison of biological finger representation from stage 3 (with exoskeleton) to stage 4 (after removal). In all line plots, perceived location (y-axis) is plotted against actual target location (x-axis). Error bars represent standard error of the mean. The dashed line indicates the identity line (slope = 1). Raincloud plots show individual participant slopes in each stage. The following figure is formatted in the same fashion.

Experiment 1B: A non-augmenting exoskeleton does not stretch the user's proprioceptive representations

We next sought to determine whether the observed training-driven representational stretch (i.e., stage 2 versus 3) was specific to training with an exoskeleton that spatially augmented the user's fingers. To this end, the same eighteen participants took part in the above experimental procedure with one change: the training was done using short exoskeletal fingers that did not meaningfully elongate the fingers (1.4 cm extension; Fig. 1A). Note that all proprioceptive mapping still included the finger-augmenting exoskeleton as in Experiment 1A. This allowed us to hold constant the mapped surface (the long extension) and time spent on the task; therefore, any stage 2 to stage 3 change could be attributed specifically to the presence of spatial augmentation during training rather than to proprioceptive mapping alone.

As in Experiment 1A, the combined bio-exoskeleton map obtained during stage 2 (initial localization with the exoskeleton) was overall geometrically accurate (true length: 17.40 cm; estimated length: 19.38 cm; paired t-test of map versus true length: $t(17) = -1.42$, $p = .17$, $BF_{10} = 0.58$). The biological finger segment was significantly under-represented relative to the exoskeletal segment (bio slope mean±sem: 0.90±0.08; exo slope mean±sem: 1.20±0.09; paired t-test: $t(17) = -3.87$, $p = .006$, $BF_{10} = 31.57$). Furthermore, comparing stage 1 (pre-exoskeleton) to stage 2, we observed that attaching the exoskeletal finger significantly contracted the represented length of the biological finger (19.37% reduction; $t(17) = 4.55$, $p = .001$, $BF_{10} = 112.87$).

We next determined the effect of using the control exoskeleton on the biological and exoskeletal finger representations. Participants were immediately fit with the finger-augmenting exoskeleton after their training with the control exoskeleton. In contrast to Experiment 1A, we did not observe changes in the length of the biological (mean±sem: 0.93±0.07, 95% CI [0.77, 1.09]; $t(17) = -0.69$, $p = 1.00$, $BF_{10} = 0.30$) or exoskeletal finger representation (mean±sem: 1.27±0.09, 95% CI [1.08, 1.45]; $t(17) = -1.68$, $p = .56$, $BF_{10} = 0.78$). This pattern suggests that proprioceptive stretch of somatosensory representations is specific to the active use of the finger-extending exoskeleton, and not simply due to the attachment or observation of them. Furthermore, although participants improved on several training tasks in this control session (e.g., pegboard, sorting, Jenga timing; see Supplementary Information), these practice gains did not translate into proprioceptive "stretching" at stage 3 when the augmenting device was fitted, indicating that the training-dependent expansion observed in Experiment 1A is augmentation-specific.

Interestingly, we replicated the effect of removing the exoskeletal fingers in stage 4. We observed a similar a modulation in the length of the participant's biological finger representation: a 20.92% increase compared to stage 1 (Fig. 3C; paired t-test: $t(17)= -4.05$, $p = .004$, $BF_{10} = 44.19$); an increase of 44.93% compared to stage 3 (Fig. 3D; paired t-test: $t(17)= -5.42$, $p < .001$, $BF_{10} = 558.70$). Intriguingly, we did not observe a significant difference between the degree of change in Experiment 1A ($t(17) = -0.36$, $p = .72$, $BF_{10} = 0.26$). These results suggest that the proprioceptive aftereffects measured in both experiments was not due to the training stage, but likely to other factors such as wearing the exoskeleton and using proprioceptive feedback of its geometry to perform the localization task. The distinct pattern of plasticity observed in both experiments after using the exoskeletons (stage 2 versus 3) and removing them (stage 4) hints at distinct internal models for the hand and hand+exoskeleton (see Discussion).

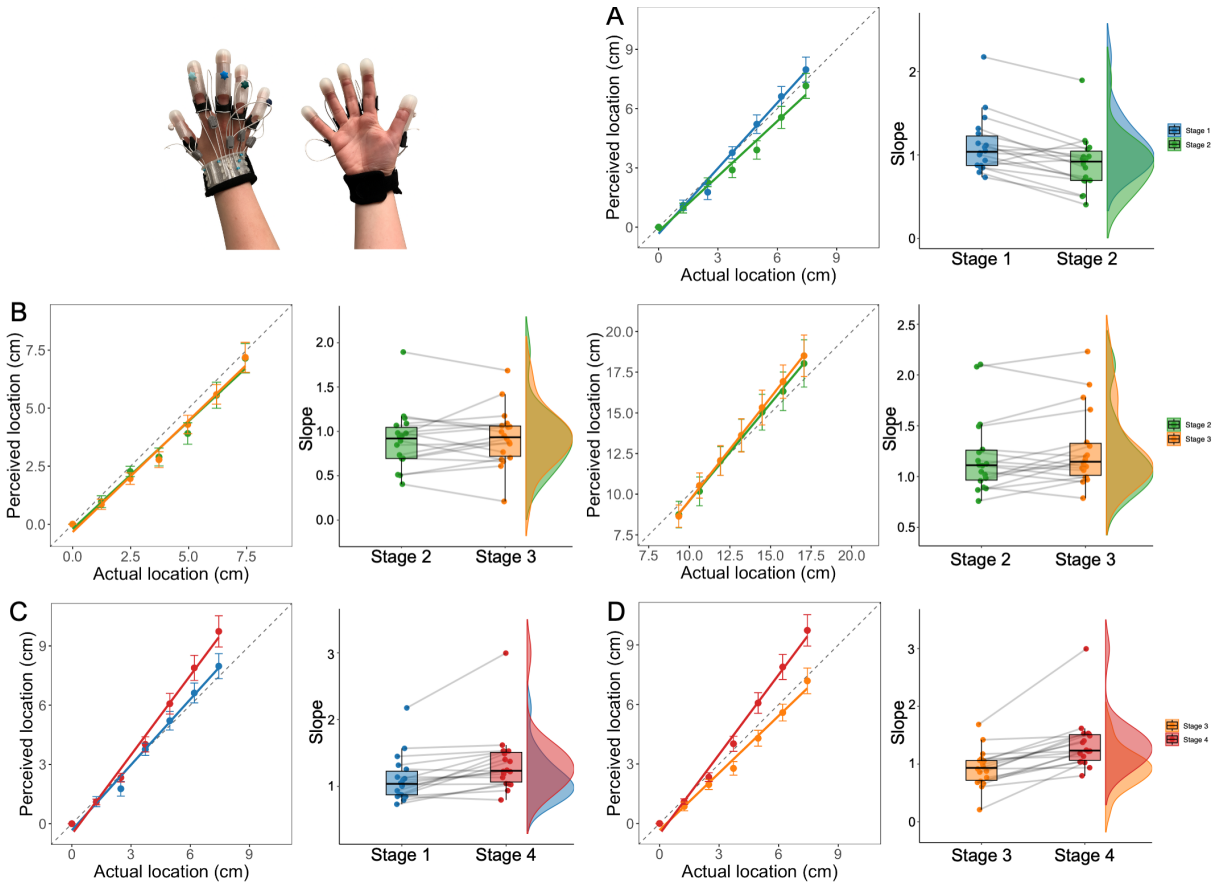

Figure 3. Proprioceptive judgments across stages with training performed using the control device. (A) Comparison of proprioceptive maps from stage 1 (baseline) and stage 2 (initial finger-extending device fitting). (B) Left: Comparison of biological finger segment between stage 2 and stage 3 (after training with control device). Right: Comparison of artificial finger segment between the same stages. (C) Comparison of biological finger representation from stage 1 to stage 4 (post-device removal). (D) Comparison of biological finger representation from stage 3 (after training with control device) to stage 4 (after removal). In all line plots, perceived location (y-axis) is plotted against actual target location (x-axis). Error bars represent standard error of the mean. The dashed line indicates the identity line (slope = 1). Raincloud plots show individual participant slopes in each stage.

Discussion

This study provides a detailed characterization of how the human somatosensory system dynamically adapts to a wearable body-augmenting exoskeleton. Using a high-density proprioceptive localization task, we show that spatial representations of both the biological body and an artificial extension can be flexibly reshaped across time. Specifically, we identified three distinct phases of somatosensory plasticity: an initial contraction of biological finger representation upon wearing the device, a functional "stretching" of both the biological and artificial finger maps following training, and a post-removal aftereffect observed at our final measurement after the exoskeleton was removed. Importantly, the emergence of these changes following training demonstrates that humans can quickly form a somatosensory representation of the exoskeleton based on sensory feedback. While the initial contraction occurred with both the finger-extending and control devices, the

functional stretching and its associated post-removal effect were specific to augmentation with an actively used, finger-extending exoskeleton. Together, our findings reveal how the somatosensory system integrates novel artificial extensions (Makin et al., 2017, 2023; Miller et al., 2019b).

We show that finger-extending exoskeletons are an effective means for investigating the dynamics of plasticity in body representations. Unlike hand-held tools, exoskeletal devices are directly interfaced with the body (Maravita and Iriki, 2004; Martel et al., 2016). Learning to use such a device introduces new demands on proprioceptive processing, requiring the integration of additional structure into the body's representational framework (Raisamo et al., 2019). Here, we observed that training with the finger-extending exoskeleton led to measurable changes in how both biological and artificial finger segments were represented. These learning-driven changes were absent when participants used a control exoskeleton that did not augment finger length, highlighting the specificity of functional engagement in driving plasticity (Biggio et al., 2020; Umiltà et al., 2008).

The initial act of wearing the exoskeleton, even before use, triggered a reallocation of representational space, leading to a contraction in the represented length of the biological finger (i.e., an under-representation). This suggests that the somatosensory system responds immediately to the presence of an artificial augmentation, even in the absence of task-specific learning. While this early "miniaturization" recalls reports from studies with passive exoskeletons (e.g., HandMorph), in which participants appeared to judge objects as larger and perceived their grasping range as reduced on first wear (Nishida et al., 2020), those findings may partly reflect task-specific factors such as altered hand posture. Nonetheless, both results point to a rapid adjustment of body representation upon donning novel augmentative devices. These observations aligns with theories of neural resource allocation, in which new sensory inputs initially compete with existing representations for limited perceptual or cortical resources (Dominijanni et al., 2021). The contraction of the biological finger's representation may reflect an adaptive mechanism, reallocating capacity toward processing novel sensorimotor structures (Makin et al., 2017; Miller et al., 2019b).

Following training, we observed that both the biological and artificial finger representations underwent a significant stretch, an effect selectively present after training with the finger-extending device and absent after control training. This parallel plasticity suggests that the brain may apply shared representational mechanisms to both body parts and technological extensions, reinforcing the idea that augmentation devices can be integrated into the sensorimotor system in a body-like manner (Makin et al., 2023, 2020; Miller et al., 2023, 2019a). The absence of such effect in the control condition emphasizes that this plasticity is not simply a response to attachment, but a specific outcome of using augmentation to achieve new functional outcomes.

One complementary way to viewing our results is via the concept of *internal models*, predictive representations of body dynamics that aid in perception and motor control (Scott, 2004; Shadmehr and Krakauer, 2008; Wolpert et al., 2001). Previous work suggests that internal models play a critical role in tool embodiment, allowing the brain to simulate and predict the outcomes of actions involving both the body and its extensions (Kilteni and Ehrsson, 2017; Miller et al., 2018). If a user forms biological+technological internal models, then motor learning should modify both similarly. Indeed, we found that the proportion of the overall representation dedicated to the biological and exoskeletal fingers remained constant before and after the observed plasticity. This suggests that the presence of a mechanism that globally stretches the representation of both surfaces, as predicted if the user learned a biological+exoskeleton internal model. This internal model likely underlies the system's ability to coordinate perception and action during interaction with the exoskeleton (Imamizu et al., 2000; Miller et al., 2018).

This biological+exoskeleton internal model appears to be newly learned during the experiment and is distinct from the user's pre-existing internal model for their fingers. Notably, simply wearing the exoskeleton led to a clear contraction of the biological finger representation, reflecting an immediate reallocation of representational space upon donning the device. This initial compression was followed by an opposite pattern once the device was removed. We observed a post-removal aftereffect—an increase in biological finger length perception following exoskeleton removal—that occurred both when participants had actively used the finger-extending exoskeleton and when they had only trained with a control device. This suggests that modifying this finger representation did not depend on motor training or functional use of the extension, as was the case with the newly learned internal model. Instead, the pre-existing internal model could be modified with repeated sensory-motor engagement involved in the proprioceptive localization task itself. Importantly, this engagement occurred while participants were still wearing the device, but its perceptual consequences became apparent only once the exoskeleton was removed and the mapping returned to the biological finger alone. Together, the initial contraction and later expansion effects indicate that wearing the device alone induces immediate representational compression, whereas only active use of the augmenting device drives the subsequent stretching observed during training.

Despite providing detailed insights into somatosensory plasticity during finger extension via exoskeleton use, our study has limitations that should be considered. The experiments were conducted under short-term, controlled conditions and did not include active sensory feedback from the device, limiting our understanding of how such plasticity unfolds in more ecologically valid or long-term contexts. Although proprioceptive localization is a high-resolution behavioral readout of body representation, it provides limited leverage on the contribution of specific sensory

channels. Systematically adding tactile or force feedback could reveal how these inputs shape the extent and form of augmentation integration. Previous studies suggest that even simple visuotactile pairing can support the embodiment of additional digits (Cadete and Longo, 2020), underscoring the potential of multisensory stimulation in shaping body representation. Moreover, recent reviews highlight that supplementary sensory feedback improves control performance and embodiment of SRLs (Pinardi et al., 2023). Therefore, these results can be relevant for the design of next-generation exoskeletons and prosthetics that incorporate artificial sensing to simulate touch. Exploring how the brain integrates these richer feedback channels could help make the artificial extensions to be experienced more like biological body parts rather than external tools. To move toward practical applications, future studies should investigate how neural representations of the finger-extending exoskeletons evolve with extended use and more complex sensorimotor feedback. These directions are essential not only for understanding sensorimotor plasticity, but also for informing the non-invasive restoration of touch in assistive technologies (Nisky and Makin, 2024).

In sum, this work demonstrates that the human sensorimotor system is capable of rapidly and flexibly integrating wearable exoskeletons into its spatial framework. Crucially, this integration is shaped by both the physical characteristics of the augmentation and the nature of the user's interaction with it. By showing that proprioceptive representations can quickly adapt to artificial extensions, we provide empirical support for the development of intuitive, body-integrated assistive technologies. Understanding the neural and perceptual mechanisms by which the brain incorporates such devices has direct implications for neurorehabilitation, prosthetics, and the design of human-machine interfaces that feel like natural extensions of the self.

Materials and Methods

Participants

A total of 20 healthy right-handed participants were recruited (mean age = 27.2 years, range = 18–54; 13 women, 7 men), all of whom completed two experimental sessions on separate days. Two participants were excluded due to the use of undesired strategies to perform the task, resulting in a final sample of 18. One used their visible left hand to mirror the position of their unseen right hand, resulting in atypically high accuracy and low uncertainty. The other switched midway from proprioceptive localization to using a fixed visual reference point, producing a bimodal response distribution. All participants had normal or corrected-to-normal vision and no history of neurological or psychiatric conditions. Participants were asked not to have long nails on the day of the experiment, as this could interfere with the usage of the exoskeleton. The research was approved by the Ethics Committee of the Faculty of Social Sciences, Radboud University. Every participant gave

informed consent to participate in the experiment. Participants were recruited through the SONA system of Radboud University and received a 30-euro voucher or course credits as compensation.

Exoskeletal fingers

The exoskeletal fingers used in this study were custom-built devices designed to augment finger function while interfacing directly with the user's hand. Each device consisted of four finger extensions and a thumb extension, mounted to a wristband. Two exoskeleton sizes, standard and large, were developed to accommodate individual differences in hand size, and an additional medium-width thumb was available for more precise fitting. Of the various size combinations, 10 participants used the small fingers with the small thumb, 8 participants used the small fingers with the medium thumb, and 2 participants used the large fingers with the medium thumb to ensure a comfortable and functionally effective fit.

The device was constructed from a combination of rigid and flexible materials. The rigid white structural components were 3D printed using PETG filament on Prusa MK3 and MK4 printers. The mechanical joints were printed in PET for greater durability. Molds for casting the outer finger surface were printed in PLA, and the surface itself was made from a skin-safe silicone mixture consisting of Wacker Elastosil Vario 15, Catalyst Vario, and silicone oil.

To cushion the user's fingers, the inner padding was cut from standard paint roller foam and secured inside the fingers using double-sided tape. Tension in the fingers was generated using standard household elastics. Tensioning components were printed in PLA. Stainless steel screws were used throughout the assembly, with nuts press-fit directly into the 3D-printed parts. The colored fingertip components were glued to the screws using superglue, and sharp plastic edges were covered with Pritt Poster Buddies for additional comfort and safety. The wristband was secured using a combination of fine-grain Velcro and standard professional-grade Velcro, sewn together to create a durable and adjustable fastening system.

The final weight of the exoskeleton varied depending on the size and thumb configuration. The standard finger extensions (without thumb) weighed 116 grams, while the large version weighed 134 grams. The thumb components weighed 28 grams (small), 32 grams (medium), and 40 grams (large). Control (non-augmenting) devices were constructed with similar dimensions but were lighter: 60 grams for standard fingers, 67 grams for large fingers, and between 11 and 15 grams for the thumb, depending on size.

Each participant was individually fitted with the appropriately sized exoskeleton. The fitting process consisted of ensuring that the finger caps were as comfortable as possible for the participant and tightening the elastic wires so that the caps were securely attached. After the exoskeleton was fitted, participants were

asked to pick up a small ball to confirm that all components were securely attached and that the device was comfortable to use.

Experimental design

Experiments 1A and 1B used a within-subject control design to isolate the effects of training with the exoskeleton on body representations. The same participants completed both sub-experiments (1A and 1B) on separate days (5–30 days apart), with the order of experiments counterbalanced across participants to mitigate between-day order effects. Each sub-experiment consisted of three parts: a touchscreen localization task, motor training, and a repetition of the localization task. A final motor task and questionnaire were also included but are not discussed in this article for brevity.

Within Experiment 1B, we deliberately trained with the short (1.4 cm) device but mapped with the long (10 cm) device both before and after training (see below). This design equates visual/proprioceptive context and total task exposure across stage 2 and stage 3 while manipulating only whether training involved true spatial augmentation. Participants were blindfolded during the brief swap to prevent visual recalibration of hand size.

High-density proprioceptive localization task

The participants were seated comfortably in a cushioned chair with their left arm resting on a padded armrest. They were positioned at a table facing the short end of a 93.2 x 52.6 cm LCD touchscreen (iiyama ProLite TF4237MSC-B3AG, Tokyo, Japan), securely fixed above the table. The right arm was placed under the screen on a board with grooves for each finger to ensure consistent placement, and participants were instructed not to look under the screen. The screen displayed three vertical stripes corresponding to the right index, middle, and ring fingers.

Localization task in the four task stages

Stage 1: The task of participants was to localize different locations on their right index finger using proprioception. The seven targets were evenly spaced between the base and fingertip along the finger's midline. Throughout the task, the participants kept their right arm completely still and made localization judgments by touching the touchscreen with their left hand (Fig. S1). After the judgment was made, they were asked to move their left hand back to the resting start position, which was 16 cm outside the response field, adjacent to the screen edge.

On a given trial, the procedure was as follows. At the beginning of the trial, an image of a finger was displayed in the lower left corner of the screen. A red dot was placed at the target location within the finger. Participants then pointed on the screen to the corresponding target location on the stripe above their actual index finger. Participants then returned their left hand to the start position. No accuracy feedback

was provided. This procedure was repeated for seven equally spaced locations across 20 trials, totaling 140 trials (see Fig. S2A for the layout of target locations). The order was randomized. This task took about 5 to 10 minutes depending on the participant's speed.

Stage 2: The proprioceptive localization task was the same as in stage 1 with the exception that participants now also localized targets within the space of the finger and the finger-augmenting exoskeleton (see Fig. S2B for the layout of the 14 target locations). There were seven distinct evenly-spaced target locations within both the biological and exoskeletal finger, for 14 distinct locations in total. There were again 20 trials per location, leading to 280 trials total. This task took around 10 to 15 minutes.

Stage 2 had the distinct procedure that it also required fitting the exoskeletal finger to the participant. After they finished the task in stage 1, they were asked to stay seated and remove their right arm from under the screen. The finger-extending exoskeleton was fitted to their right hand for both experimental and control sessions. After making sure the exoskeleton fit comfortably, the participants' right arm was placed under the screen again in the same position as before.

In Experiment 1A, the participants continued with the finger-extending exoskeleton. In Experiment 1B, after finishing both localization tasks, the finger-extending exoskeleton was removed, and the control exoskeleton was fitted in the same way as the finger-extending exoskeleton.

Stage 3: After completing the motor tasks (see "Training protocol" below), participants were guided back to the touchscreen to repeat the localization task, which was the same proprioceptive localization task as in stage 2. In Experiment 1B, before starting this task, the control exoskeleton was replaced with the finger-extending exoskeleton while the participant was blindfolded. The blindfold ensured that participants did not see their hand without the exoskeleton, preventing visual input from recalibrating their hand representation and potentially diminishing the effects of the training. In Experiment 1A participants remained wearing the exoskeletal finger.

Stage 4: For the finger-only localization task, the exoskeleton was removed while participants were blindfolded, and their hand was guided back under the screen before the blindfold was removed. Participants then performed the same proprioceptive localization task as in stage 1.

Training protocol

The training took place between stages 2 and 3. During the training, participants were asked to complete a set of tasks to familiarize them with the use of the exoskeletal fingers and train their motor control. They were instructed that the tasks should be completed predominantly with their right, exoskeleton-wearing hand. That is, grasping and manipulation was to be performed solely with the right hand, and they were to only use their left hand in a supportive role when needed, that is, only to

stabilize objects or assist minimally without performing the main action. This approach was chosen to make the training more ecologically relevant, as in daily life, both hands would typically be used to complete such tasks. Each task was repeated three times, forming three blocks of trials. Within each block, the order of tasks was consistent for each participant, but this order was randomized across participants.

The tasks included in the training were based on a previously introduced protocol (Kieliba et al., 2021): building a Jenga tower with wooden blocks, sorting plastic bricks according to their color, and sorting shapes by inserting them into a wooden box. In addition, participants completed the Purdue Pegboard Test (both long and short peg versions) before and after the three repetitions (Lawson, 2019). See the Supplementary Information for a detailed description of each task.

Data analysis

The data were tested for normality using the Shapiro–Wilk test and found to be normally distributed ($p > .05$); therefore, parametric statistics were used. Linear regression was used to quantify the represented length of finger and exoskeleton. In the localization tasks, the perceived location of each target was calculated as the mean of participants' response distributions. The true position of the targets was determined from participants' finger measurements and the known exoskeleton length. By performing regressions of perceived versus true locations, we obtained an offset (β_0) and a slope (β_1). The offset was discarded, as it only reflected a spatial bias without providing information on length perception. The slope, however, indicates the scaling factor and represents participants' length perception.

For the finger-only localization task, one regression was performed per condition (pre- and post-training), resulting in four slopes per participant (two per sub-experiment). For the finger+exoskeleton localization task, two regressions were performed per condition (pre- and post-training): one for the biological finger segment and one for the exoskeleton segment, yielding eight slopes per participant. These slopes quantified perceived spatial scaling along each segment and served as a measure of perceived length.

The comparison of the represented length involved analyzing the segments separately, leading to two comparisons of condition and pre/post-training. Changes in slope across experimental stages (e.g., before and after training) were evaluated using paired t-tests. We conducted planned comparisons between stage 1 vs. 2 (finger), 2 vs. 3 (finger and exoskeleton), 1 vs. 4 (finger), 3 vs. 4 (finger) within each of Experiment 1A and 1B, resulting in five paired t-tests per experiment. Reported p-values were Bonferroni-corrected within each experiment to account for five planned comparisons.

All p-values are two-tailed and are reported alongside 95% confidence intervals and Bayes Factors (BFs). For Bayesian analyses, the default Cauchy prior was used.

References

Abdi E, Burdet E, Bouri M, Himidan S, Bleuler H. 2016. In a demanding task, three-handed manipulation is preferred to two-handed manipulation. *Sci Rep* **6**:21758.

Berti A, Frassinetti F. 2000. When far becomes near: remapping of space by tool use. *J Cogn Neurosci* **12**:415–420.

Biggio M, Bisio A, Avanzino L, Ruggeri P, Bove M. 2020. Familiarity with a tool influences peripersonal space and primary motor cortex excitability of muscles involved in haptic contact. *Cereb Cortex Commun* **1**:tgaa065.

Bruno V, Carpinella I, Rabuffetti M, De Giuli L, Sinigaglia C, Garbarini F, Ferrarin M. 2019. How tool-use shapes body metric representation: Evidence from motor training with and without robotic assistance. *Front Hum Neurosci* **13**:299.

Cadete D, Longo MR. 2020. A continuous illusion of having a sixth finger. *Perception* **49**:807–821.

Canzoneri E, Ubaldi S, Rastelli V, Finisguerra A, Bassolino M, Serino A. 2013. Tool-use reshapes the boundaries of body and peripersonal space representations. *Exp Brain Res* **228**:25–42.

Cardinali L, Brozzoli C, Urquizar C, Salemme R, Roy AC, Farnè A. 2011. When action is not enough: tool-use reveals tactile-dependent access to Body Schema. *Neuropsychologia* **49**:3750–3757.

Cardinali L, Frassinetti F, Brozzoli C, Urquizar C, Roy AC, Farnè A. 2009. Tool-use induces morphological updating of the body schema. *Curr Biol* **19**:R478-9.

Debats NB, Ernst MO, Heuer H. 2017. Perceptual attraction in tool use: evidence for a reliability-based weighting mechanism. *J Neurophysiol* **117**:1569–1580.

Dominijanni G, Shokur S, Salvietti G, Buehler S, Palmerini E, Rossi S, De Vignemont F, d'Avella A, Makin TR, Prattichizzo D, Micera S. 2021. The neural resource allocation problem when enhancing human bodies with extra robotic limbs. *Nat Mach Intell* **3**:850–860.

Dowdall L, Molina-Sanchez M, Dominijanni G, da Silva E, Pavalkyte V, Jugovic E, Bianchi M, Iida F, Clode D, Makin TR. 2025. Developing a sensory representation of an artificial body part. *bioRxiv*. doi:10.1101/2025.06.16.658246

Eden J, Bräcklein M, Ibáñez J, Barsakcioglu DY, Di Pino G, Farina D, Burdet E, Mehring C. 2022. Principles of human movement augmentation and the challenges in making it a reality. *Nat Commun* **13**:1345.

Fabio C, Salemme R, Farnè A, Miller LE. 2024. Alpha oscillations reflect similar mapping mechanisms for localizing touch on hands and tools. *iScience* **27**:109092.

Galigani M, Castellani N, Donno B, Franza M, Zuber C, Allet L, Garbarini F, Bassolino M. 2020. Effect of tool-use observation on metric body representation and peripersonal space. *Neuropsychologia* **148**:107622.

Gallivan JP, McLean DA, Valyear KF, Culham JC. 2013. Decoding the neural mechanisms of human tool use. *Elife* **2**:e00425.

Garbarini F, Fossataro C, Berti A, Gindri P, Romano D, Pia L, della Gatta F, Maravita A, Neppi-Modona M. 2015. When your arm becomes mine: pathological embodiment of alien limbs using tools modulates own body representation. *Neuropsychologia* **70**:402–413.

Holmes NP, Spence C. 2004. The body schema and the multisensory representation(s) of peripersonal space. *Cogn Process* **5**:94–105.

Hussain I, Salvietti G, Spagnoletti G, Prattichizzo D. 2016. The soft-SixthFinger: A wearable EMG controlled robotic extra-finger for grasp compensation in chronic stroke patients. *IEEE Robot Autom Lett* **1**:1000–1006.

Imamizu H, Miyauchi S, Tamada T, Sasaki Y, Takino R, Pütz B, Yoshioka T, Kawato M. 2000. Human cerebellar activity reflecting an acquired internal model of a new tool. *Nature* **403**:192–195.

Iriki A, Tanaka M, Iwamura Y. 1996. Coding of modified body schema during tool use by macaque postcentral neurones. *Neuroreport* **7**:2325–2330.

Kieliba P, Clode D, Maimon-Mor RO, Makin TR. 2021. Robotic hand augmentation drives changes in neural body representation. *Sci Robot* **6**. doi:10.1126/scirobotics.abd7935

Kilteni K, Ehrsson HH. 2017. Sensorimotor predictions and tool use: Hand-held tools attenuate self-touch. *Cognition* **165**:1–9.

Lawson I. 2019. Purdue pegboard test. *Occup Med (Lond)* **69**:376–377.

Longo MR, Serino A. 2012. Tool use induces complex and flexible plasticity of human body representations. *Behav Brain Sci*.

Maekawa A, Kawamura K, Inami M. 2020. Dynamic assistance for human balancing with inertia of a wearable robotic appendage2020 IEEE/RSJ International Conference on Intelligent Robots and Systems (IROS). Presented at the 2020 IEEE/RSJ International Conference on Intelligent Robots and Systems (IROS). IEEE. doi:10.1109/iros45743.2020.9341323

Makin TR, de Vignemont F, Faisal AA. 2017. Neurocognitive barriers to the embodiment of technology. *Nat Biomed Eng* **1**:0014.

Makin TR, de Vignemont F, Micera S. 2020. Soft embodiment for engineering artificial limbs. *Trends Cogn Sci* **24**:965–968.

Makin TR, Micera S, Miller LE. 2023. Neurocognitive and motor-control challenges for the realization of bionic augmentation. *Nat Biomed Eng* **7**:344–348.

Maravita A, Iriki A. 2004. Tools for the body (schema). *Trends Cogn Sci* **8**:79–86.

Martel M, Cardinali L, Bertonati G, Jouffrais C, Finos L, Farnè A, Roy AC. 2019. Somatosensory-guided tool use modifies arm representation for action. *Sci Rep* **9**:5517.

Martel M, Cardinali L, Roy AC, Farnè A. 2016. Tool-use: An open window into body representation and its plasticity. *Cogn Neuropsychol* **33**:82–101.

Miller LE, Cawley-Bennett A, Longo MR, Saygin AP. 2017. The recalibration of tactile perception during tool use is body-part specific. *Exp Brain Res* **235**:2917–2926.

Miller LE, Fabio C, de Vignemont F, Roy A, Medendorp WP, Farnè A. 2023. A somatosensory computation that unifies limbs and tools. *eNeuro* **10**:ENEURO.0095-23.2023.

Miller LE, Fabio C, Ravenda V, Bahmad S, Koun E, Salemme R, Luauté J, Bolognini N, Hayward V, Farnè A. 2019a. Somatosensory cortex efficiently processes touch located beyond the body. *Curr Biol* **29**:4276-4283.e5.

Miller LE, Farnè A. 2024. Extending Tactile Space With Handheld Tools: A Re-Analysis and Review **1**:1–19.

Miller LE, Longo MR, Saygin AP. 2019b. Tool use modulates somatosensory cortical processing in humans. *J Cogn Neurosci* **31**:1782–1795.

Miller LE, Longo MR, Saygin AP. 2014. Tool morphology constrains the effects of tool use on body representations. *J Exp Psychol Hum Percept Perform* **40**:2143–2153.

Miller LE, Montroni L, Koun E, Salemme R, Hayward V, Farnè A. 2018. Sensing with tools extends somatosensory processing beyond the body. *Nature* **561**:239–242.

Mooney LM, Herr HM. 2016. Biomechanical walking mechanisms underlying the metabolic reduction caused by an autonomous exoskeleton. *J Neuroeng Rehabil* **13**:4.

Najafabadi AJ, Küster D, Putze F, Godde B. 2023. Emergence of sense of body ownership but not agency during virtual tool-use training is associated with an altered body schema. *Exp Brain Res* **241**:1721–1738.

Nishida J, Matsuda S, Matsui H, Teng S-Y, Liu Z, Suzuki K, Lopes P. 2020. HandMorph: a Passive Exoskeleton that Miniaturizes GraspProceedings of the 33rd Annual ACM Symposium on User Interface Software and Technology. Presented at the UIST '20: The 33rd Annual ACM Symposium on User Interface Software and Technology. New York, NY, USA: ACM. doi:10.1145/3379337.3415875

Nisky I, Makin TR. 2024. A neurocognitive pathway for engineering artificial touch. *Sci Adv* **10**:eadq6290.

Penaloza CI, Nishio S. 2018. BMI control of a third arm for multitasking. *Sci Robot* **3**:eaat1228.

Peviani VC, Pfeifer LN, Risso G, Bassolino M, Miller LE. 2024. Tool use fine-tunes arm and tool maps. *bioRxiv*. doi:10.1101/2024.06.06.597694

Pinardi M, Longo MR, Formica D, Strbac M, Mehring C, Burdet E, Di Pino G. 2023. Impact of supplementary sensory feedback on the control and embodiment in human movement augmentation. *Commun Eng* **2**. doi:10.1038/s44172-023-00111-1

Prattichizzo D, Pozzi M, Lisini Baldi T, Malvezzi M, Hussain I, Rossi S, Salvietti G. 2021. Human augmentation by wearable supernumerary robotic limbs: review and perspectives. *Prog Biomed Eng (Bristol)* **3**:042005.

Raisamo R, Rakkolainen I, Majaranta P, Salminen K, Rantala J, Farooq A. 2019. Human augmentation: Past, present and future. *Int J Hum Comput Stud* **131**:131–143.

Romano D, Uberti E, Caggiano P, Cocchini G, Maravita A. 2019. Different tool training induces specific effects on body metric representation. *Exp Brain Res* **237**:493–501.

Scott SH. 2004. Optimal feedback control and the neural basis of volitional motor control. *Nat Rev Neurosci* **5**:532–546.

Shadmehr R, Krakauer JW. 2008. A computational neuroanatomy for motor control. *Exp Brain Res* **185**:359–381.

Shafti A, Haar S, Mio R, Guilleminot P, Faisal AA. 2021. Playing the piano with a robotic third thumb: assessing constraints of human augmentation. *Sci Rep* **11**:21375.

Solomon HY, Turvey MT. 1988. Haptically perceiving the distances reachable with hand-held objects. *J Exp Psychol Hum Percept Perform* **14**:404–427.

Sposito A, Bolognini N, Vallar G, Maravita A. 2012. Extension of perceived arm length following tool-use: clues to plasticity of body metrics. *Neuropsychologia* **50**:2187–2194.

Themelis LZ, Medendorp WP, Miller LE. 2025. Gaze-centered spatial coding of touch on a hand-held tool. *bioRxiv*. doi:10.1101/2025.04.04.647167

Umezawa K, Suzuki Y, Ganesh G, Miyawaki Y. 2022. Bodily ownership of an independent supernumerary limb: an exploratory study. *Sci Rep* **12**:2339.

Umiltà MA, Escola L, Intskirveli I, Grammont F, Rochat M, Caruana F, Jezzini A, Gallese V, Rizzolatti G. 2008. When pliers become fingers in the monkey motor system. *Proc Natl Acad Sci U S A* **105**:2209–2213.

Wolpert DM, Ghahramani Z, Flanagan JR. 2001. Perspectives and problems in motor learning. *Trends Cogn Sci* **5**:487–494.

Yang B, Huang J, Chen X, Xiong C, Hasegawa Y. 2021. Supernumerary robotic limbs: A review and future outlook. *IEEE Trans Med Robot Bionics* **3**:623–639.

Acknowledgments: We would like to thank Sibrecht Bouwstra for her key role in the development of the exoskeletons, as well as the Technical Support Group of the Donders Centre for Cognition for their additional support. **Funding:** This research was supported by a European Research Council Starting Grant (ERC 101076991 SOMATOGPS) and Dutch Research Council VIDI Grant (VI.VIDI.221G.02) to LEM. The funding sources were involved in study design, data collection and interpretation, or the decision to submit the work for publication. **Author contributions:** Conceptualization: DR, SG, VCP, LEM; Methodology: DR, SG, VCP, LEM; Investigation: SG; Visualization: DR, SG; Supervision: VCP, LEM; Writing—original draft: DR, LEM; Writing—review & editing: DR, SG, VCP, LEM. **Competing interests:** Authors declare that they have no competing interests. **Data and materials availability:** The data and code that support the findings of this study will be available from the Open Science Framework upon publication.

Supplementary Materials for

Dynamics of sensorimotor plasticity during exoskeletal finger augmentation

Dominika Radziun* *et al.*

*Corresponding author. Email: dominika.radziun@donders.ru.nl

This PDF file includes:

Supplementary experimental and analytical details
Experimental setup for localization task
Training task descriptions and outcome measures

Supplementary experimental and analytical details

Experimental setup for localization task

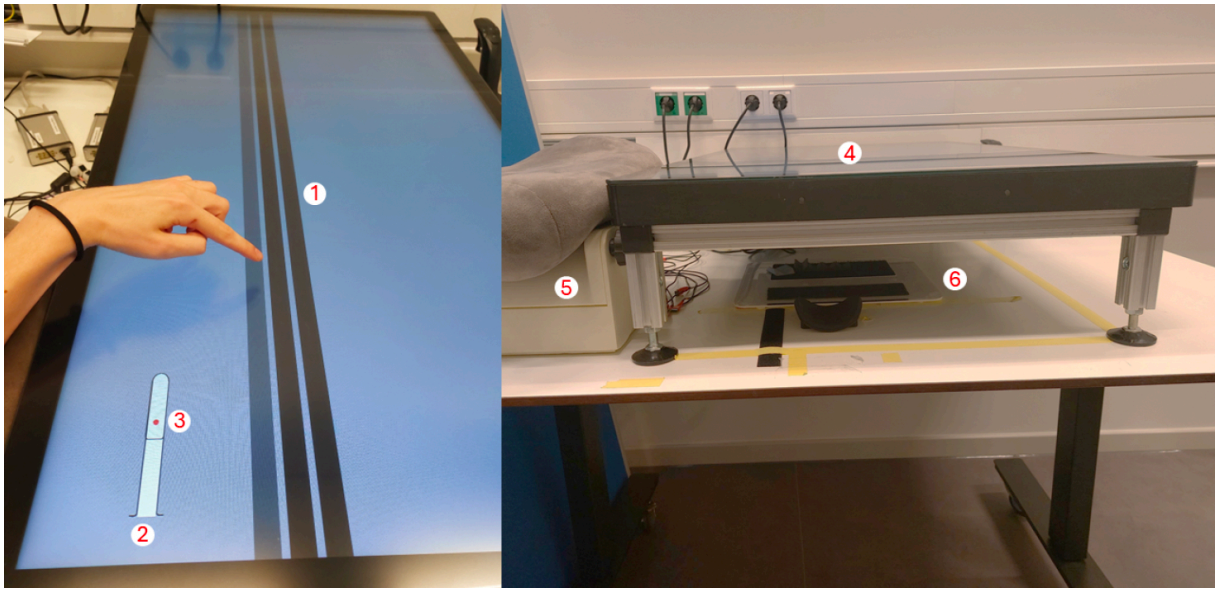

Figure S1. A top-down view of the finger+exoskeleton localization task (left) and a frontal view of the localization task setup (right). (1) The three stripes are aligned with the index, middle, and ring fingers placed under the touchscreen. The left stripe is colored in gray to indicate the finger of interest. (2) The image of a finger with the exoskeleton shown to the participant on which the requested locations are displayed. (3) One of the 14 requested locations displayed on the finger in red. (4) The elevated touchscreen under which the right hand is placed. (5) The elevated armrest on which the right elbow is placed. (6) The board with the finger grooves on which the right hand is placed together with a small armrest for the forearm.

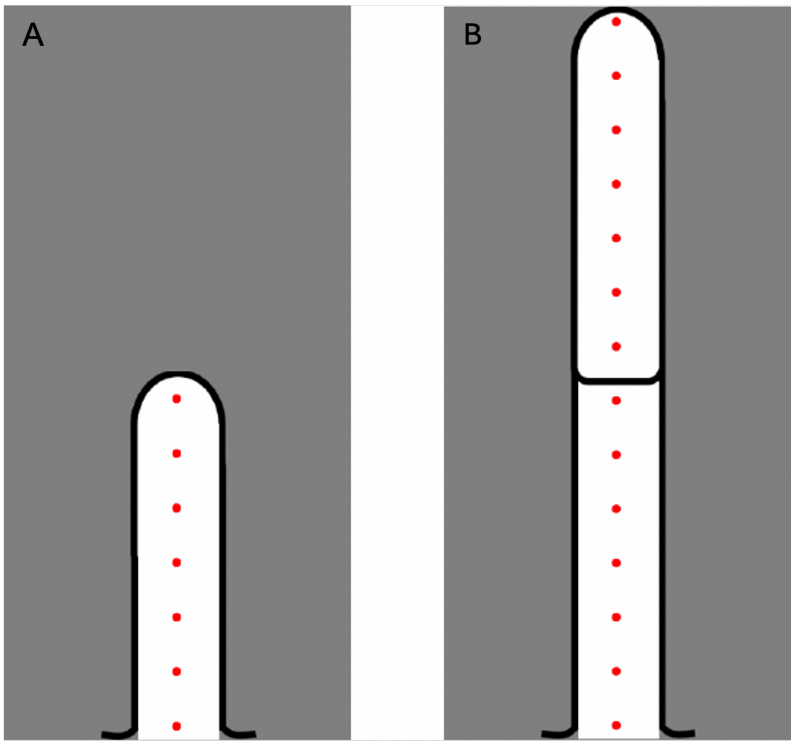

Figure S2. The distribution of 7 locations for the finger (A) and 14 locations for the finger+exoskeleton (B) localization tasks.

Training task descriptions and outcome measures

Following the 30–45 minutes training period, participants' performance with the exoskeletal fingers was assessed across multiple tasks. Detailed statistical analyses confirmed a significant learning effect over time.

Task completion times (the primary outcome measure) were assessed for normality using the Shapiro–Wilk test. When any repetition within a task significantly deviated from normality, the entire task was analyzed using a non-parametric method (Wilcoxon signed-rank test); otherwise, parametric methods were applied. Planned pairwise comparisons were conducted between blocks (block 1 vs. block 2, block 2 vs. block 3) using two-tailed tests. Statistical comparisons involving were evaluated against a Bonferroni-adjusted significance threshold of $\alpha = 0.025$ to account for multiple planned comparisons.

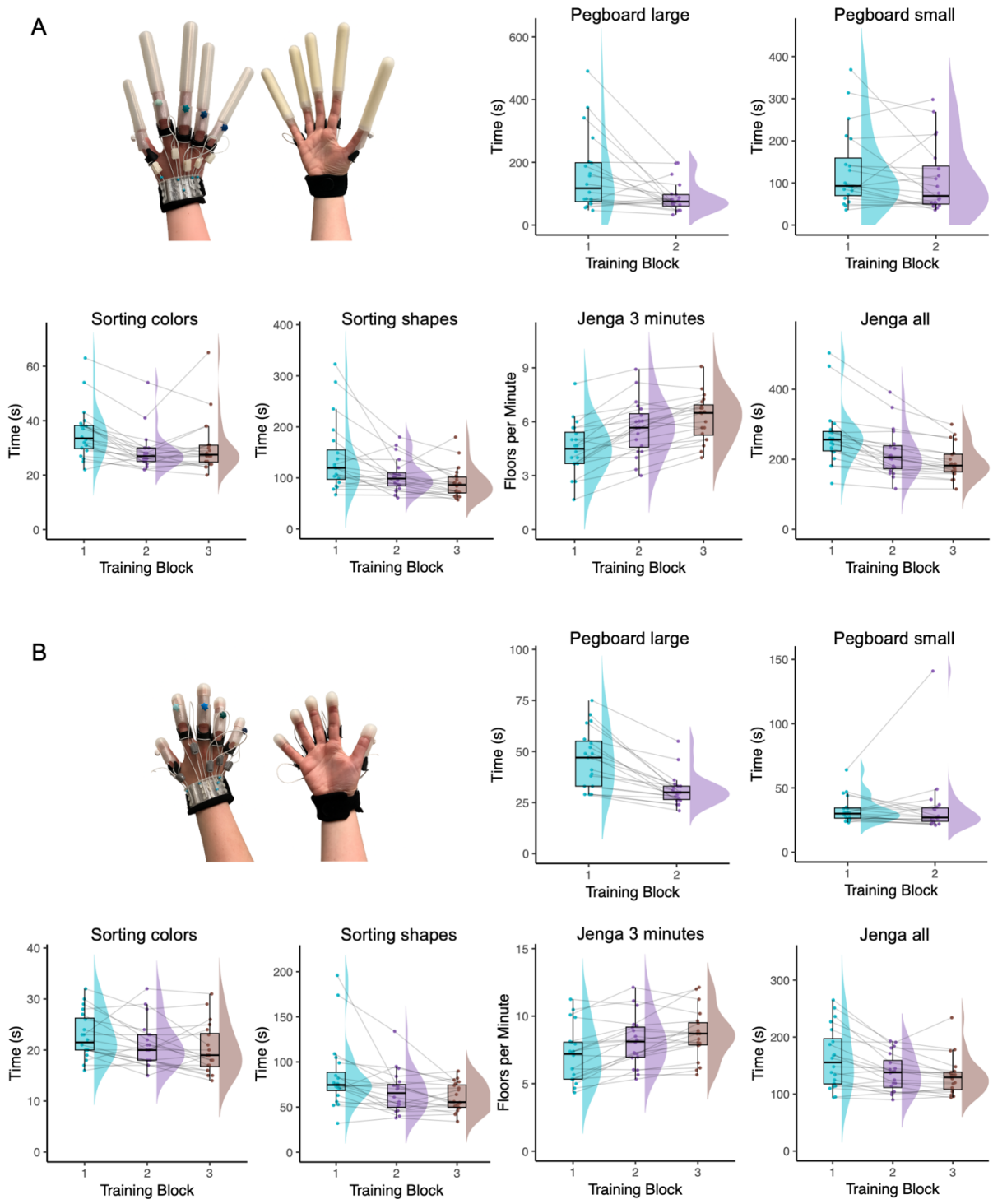

Figure S3. Overview of training tasks performed in Experiment 1A (A) and Experiment 1B (B). In Experiment 1A, participants trained with a finger-extending exoskeleton; in Experiment 1B, participants trained with a control, non-extending device. Each panel displays two rows of task conditions: the top row shows the pegboard transfer tasks with large and small pegs, and the bottom row shows the sorting colors task, sorting shapes task, the Jenga 3-minute task, and the Jenga all task.

Pegboard transfer task

Before and after the training, participants completed a custom task inspired by the Purdue pegboard task. The task was divided into two stages: one involving larger pegs (9 cm long) and one involving smaller pegs (5 cm long), both with a diameter of 0.7 cm at the ends and 0.8 cm at the midpoint. All pegs were made from standard PVC stock and lathed at the ends for improved grip. Participants were asked to transfer 14 pegs from one wooden pegboard to another, using only their right hand, which was fitted with the exoskeleton. The pegboard featured 27 holes arranged in 9 rows and 3 columns. Grasping and manipulation were to be performed solely with the right hand, while the left hand was allowed only to stabilize the pegboard. The outcome measure was the time taken to complete the transfer.

In Experiment 1A, which involved training with the finger-extending exoskeleton, participants showed significant improvements in the large peg condition. Completion times were significantly reduced following the training session (Wilcoxon $V(19) = 27.0$, $p = .006$, $BF_{10} = 5.67$), indicating improved gross motor performance. Performance in the small peg condition did not improve significantly (Wilcoxon $V(19) = 59.0$, $p = .09$, $BF_{10} = 0.56$).

In Experiment 1B, which involved training with a control, non-extending device, participants significantly improved their performance in the large peg condition (Wilcoxon $V(18) = 0.0$, $p < .001$, $BF_{10} = 2185.93$). No significant change was found in the small peg condition (Wilcoxon $V(18) = 56.5$, $p = .206$, $BF_{10} = 0.25$). Excluding one outlier due to a technical issue with the coating on the device's fingertips did not alter the outcome (Wilcoxon $V(17) = 38.5$, $p = .13$, $BF_{10} = 0.42$). Due to a technical issue that completely prevented one participant from completing the task in the post-training session, the initial total number of participants for this analysis was 19 instead of 20.

Sorting colors task

In the *sorting colors task*, participants were asked to sort LEGO® DUPLO® bricks into plastic trays according to color, using only their right hand, which was equipped with the exoskeleton. The task involved four colors, yellow, red, green, and blue, and included a fixed number of bricks in two standard sizes. The set comprised two large yellow bricks, one small yellow brick, three large red bricks, six small red bricks, one large green brick, two small green bricks, one large blue brick, and three small blue bricks. Small bricks measured 32 mm × 32 mm in width and depth, with a height of 19.2 mm (22 mm including studs), while the large bricks were 32 mm wide, 64 mm long, and approximately the same height. The outcome measure was the time required to complete the task.

In Experiment 1A, participants trained with the functional finger-extending exoskeleton showed a significant improvement in sorting performance following the initial training session. Task completion time decreased significantly from session 1 to session 2 (Wilcoxon $V(19) = 8.5$, $p = .006$, $BF_{10} = 2782.66$), indicating a rapid learning effect. However, no further improvement was observed between session 2 and session 3 (Wilcoxon $V(19) = 61.5$, $p = .95$, $BF_{10} = 0.397$), suggesting that most of the learning occurred early in the training and plateaued thereafter.

In Experiment 1B, participants using the control device did not show statistically significant improvement between session 1 and session 2 (Wilcoxon $V(19) = 31.0$, $p = .06$, $BF_{10} = 1.24$), nor between session 2 and session 3 (Wilcoxon $V(19) = 49.0$, $p = .38$, $BF_{10} = 0.47$). This indicates that training with the control device did not lead to measurable performance enhancement across sessions, in contrast to the group using the finger-extending exoskeleton.

Sorting shapes task

In the *sorting shapes task*, participants were asked to insert wooden blocks into their corresponding holes in a wooden shape-sorting box. The set included 16 uniquely shaped and colored blocks: a yellow rhombus, yellow trapezoid, yellow pentagon, red triangle, red trapezoid, red hexagon, green square, green rectangle, green octagon, blue oval, blue star, and blue flower. Each shape was represented once. Participants were instructed to carry out all grasping and manipulation with their right, exoskeleton-wearing hand, while the left hand could be used only to support or reposition the box if needed. The outcome measure was the time taken to insert all shapes correctly into their respective slots.

In Experiment 1A, involving the finger-extending exoskeleton, participants demonstrated significant improvements in task performance across sessions. Completion time decreased significantly from session 1 to session 2 (Wilcoxon $V(19) = 32.0$, $p = .01$, $BF_{10} = 5.52$), suggesting that the device supported the development of improved control and efficiency during shape manipulation. A further improvement was observed from session 2 to session 3 (Wilcoxon $V(19) = 36.0$, $p = .036$, $BF_{10} = 1.50$), indicating continued performance gains with additional practice.

In Experiment 1B, where participants trained with the control device, significant improvement was observed between session 1 and session 2 (Wilcoxon $t(19) = 29.5$, $p = .01$, $BF_{10} = 3.70$). However, no further improvement occurred from session 2 to session 3 (Wilcoxon $t(19) = 66.0$, $p = .31$, $BF_{10} = 0.74$). This pattern indicates that while early gains occurred in both experimental contexts, ongoing improvements were specific to training with the finger-extending exoskeleton.

Jenga 3-minute task

In the *Jenga 3-minute task*, participants were instructed to build as many complete floors of a Jenga tower as possible within a fixed time limit of three minutes. Each floor consisted of three standard rectangular wooden blocks placed side by side. Participants used only their right hand, equipped with the exoskeleton, to manipulate and place the blocks. The left hand was not permitted during the task. The primary outcome measure was the number of full floors completed within the three-minute window.

In Experiment 1A, where participants trained with the finger-extending exoskeleton, performance improved significantly across sessions. The number of completed floors increased from session 1 to session 2 ($t(19) = -5.98$, $p < .001$, $BF_{10} = 2343.80$), and further gains were observed from session 2 to session 3 ($t(19) = -4.31$, $p < .001$, $BF_{10} = 86.28$). These results suggest that participants became progressively more efficient at using the device for the task, benefiting from both initial learning and continued refinement over multiple training blocks.

In Experiment 1B, conducted with the control device, participants also showed a significant improvement between session 1 and session 2 ($t(19) = -4.70$, $p < .001$, $BF_{10} = 188.06$). However, no statistically significant improvement was observed between session 2 and session 3 ($t(19) = -2.43$, $p = .05$, $BF_{10} = 2.40$). This pattern shows that sustained gains across sessions were more pronounced in the context of training with the active exoskeleton.

Jenga all task

In the *Jenga all task*, participants were asked to build a complete Jenga tower consisting of 18 floors, with each floor made up of three wooden blocks. Unlike the 3-minute version, this task required the tower to be completed in its entirety, regardless of how long it took. As in the other tasks, participants were instructed to use only their right hand, which was fitted with the

exoskeleton, to manipulate and place the blocks. The left hand was not permitted. The outcome measure was the total time required to complete the full tower.

In Experiment 1A, which involved training with the finger-extending exoskeleton, participants showed significant improvement across sessions. Completion times decreased between session 1 and session 2 (Wilcoxon $t(19) = 1.0$, $p < .001$, $BF_{10} = 974.07$), and continued to improve from session 2 to session 3 (Wilcoxon $t(19) = 8.0$, $p < .001$, $BF_{10} = 30.45$). These results indicate consistent gains in efficiency when using the finger-extending exoskeleton, suggesting ongoing refinement with repeated use of the device.

In Experiment 1B, when participants performed the training using the control device, a significant reduction in completion time was also observed from session 1 to session 2 (Wilcoxon $t(19) = 22.5$, $p = .002$, $BF_{10} = 45.24$). However, no significant improvement was found between session 2 and session 3 (Wilcoxon $t(19) = 51.0$, $p = .08$, $BF_{10} = 0.68$). As with the 3-minute task, this suggests that while initial exposure to the task led to performance gains under both experimental contexts, continued improvement was more robust and sustained in the presence of active device support.